Am J Transl Res 2024;16(8):3654-3666
www.ajtr.org /ISSN:1943-8141/AJTR0157325

Original Article

Efficacy of color Doppler ultrasound signs combined with serum tumor-specific growth factor in the diagnosis of differentiated thyroid cancer

Xin Chen[1], Xin Gao[1], Xiaoxiao Ma[1], Bao Wei[2], Mihong Bai[3]

[1]Department of Ultrasound, Yulin Hospital, The First Affiliated Hospital of Xi'an Jiaotong University, The Intersection of Wenhua South Road and Kang'an Road, Yuyang District, Yulin 719000, Shaanxi, China; [2]Department of Thoracic Surgery, Baoji People's Hospital, No. 24 Xinhua Lane, Jing'er Road, Weibin District, Baoji 721000, Shaanxi, China; [3]Department of Laboratory, Baoji People's Hospital, No. 24 Xinhua Lane, Jing'er Road, Weibin District, Baoji 721000, Shaanxi, China

Received April 21, 2024; Accepted June 8, 2024; Epub August 15, 2024; Published August 30, 2024

Abstract: Objective: To construct a diagnostic model for follicular thyroid carcinoma (FTC) and papillary thyroid carcinoma (PTC), both subtypes of differentiated thyroid carcinoma (DTC), using color Doppler ultrasound signs in conjunction with serum laboratory markers. Methods: We conducted a retrospective analysis of patients with thyroid nodules who underwent ultrasonography at Yulin Hospital from February 2021 to March 2023. The cohort included 269 subjects: 105 with benign nodules and 164 with DTC (59 with FTC and 105 with PTC). We compared baseline demographics and laboratory indices between the groups. Diagnostic values of ultrasound features and laboratory markers were assessed using receiver operating characteristic (ROC) curves, and logistic regression was employed to pinpoint independent diagnostic factors for FTC. A predictive nomogram was subsequently developed based on these factors. Results: There were significant differences between the benign and malignant groups regarding ultrasound signs (including border, morphology, echogenicity, calcification, blood flow, lymph node zoning) and laboratory indices (free triiodothyronine (FT3), free thyroxine (FT4), thyroglobulin (Tg), thyroid-stimulating hormone (TSH), vascular endothelial growth factor (VEGF), tumor-specific growth factor (TSGF)), with all *P*-values <0.05. The areas under the curve (AUCs) for FT3, FT4, Tg, TSH, VEGF, and TSGF were all above 0.75, with Tg achieving the highest at 0.91. Logistic regression identified borders, morphology, echogenicity, VEGF, and TSGF as independent diagnostic factors for distinguishing between FTC and PTC, with significant *P*-values. The constructed nomogram demonstrated an AUC of 0.853, indicating high diagnostic accuracy. Both calibration and decision curve analysis (DCA) validated the model's stability and clinical utility. Conclusion: We successfully developed a nomogram combining ultrasound features and serum markers that enhances the diagnostic precision for FTC. This model offers a valuable tool for clinical diagnostics in differentiated thyroid cancer.

Keywords: Color Doppler ultrasound, tumor-specific growth factor, differentiated thyroid cancer, diagnosis

Introduction

Thyroid cancer (TC), originating from the follicular or parafollicular epithelial cells of the thyroid gland, is among the top ten most common malignant tumors [1]. It includes various histologic types such as papillary thyroid carcinoma (PTC), follicular thyroid carcinoma (FTC), medullary thyroid carcinoma (MTC), and anaplastic thyroid carcinoma (ATC) [2]. PTC, the most prevalent type, accounts for approximately 60% to 70% of all thyroid cancers and primarily affects young females, with 50% to 80% of cases occurring in patients under 40 years of age [3]. PTC typically exhibits slow growth and lower malignancy but tends to metastasize early to local lymph nodes. Conversely, FTC represents about 20% to 25% of cases and is associated with higher malignancy and poorer prognosis [4].

Doppler color ultrasound, a non-invasive, radiation-free diagnostic technique, is extensively used to assess thyroid nodules [5]. It is crucial for detecting differentiated thyroid cancer (DTC), providing detailed information on the

https://doi.org/10.62347/GARM5333

blood flow characteristics within the nodules, such as presence, velocity, and distribution of flow [6]. This imaging modality is particularly valuable for identifying DTC subtypes like PTC and FTC by monitoring dynamic blood flow changes in these nodules, offering important diagnostic insight [7]. However, reliance solely on imaging features may lead to misdiagnoses or underdiagnoses, as it does not assess the overall condition of the patient comprehensively [8]. Thus, while Doppler color ultrasound is instrumental for initial screening and diagnosing DTC, its accuracy and specificity for diagnosing PTC and FTC need further improvement.

Vascular endothelial growth factor (VEGF) is a cytokine primarily involved in angiogenesis [9]. It is known that tumor cells enhance angiogenesis by secreting VEGF, thereby supplying essential nutrients and oxygen necessary for tumor growth and dissemination [10]. As a result, VEGF expression levels are frequently used as biomarkers for assessing the invasiveness and metastatic potential of tumors. Tumor-specific growth factors (TSGF) are a group of substances that specifically promote tumor angiogenesis and the formation of vascular networks [11]. TSGF plays a pivotal role in the tumor microenvironment by influencing vascularization, and aiding tumor cell proliferation, migration, and immune evasion [12]. Notably, variations in TSGF activity and expression levels across different tumor types are significant, critically affecting tumor development and prognostic assessment. Both VEGF and TSGF regulate angiogenesis and tumor progression, with VEGF mainly facilitating the formation of new blood vessels, and TSGF enhancing the tumor's vascular network to support growth. Research has demonstrated a positive correlation between serum and tissue levels of these factors, suggesting that serum concentrations can reflect tissue levels and overall angiogenic activity within tumors [13].

Although various indicators have been used in diagnosing benign nodules and DTC, no studies have conclusively shown that combining ultrasound signs with laboratory indicators significantly enhances diagnostic efficacy [14]. Nevertheless, recent years have seen considerable effort in developing and refining diagnostic models for thyroid nodules [15]. This study aims to equip clinicians with a more accurate diagnostic tool by developing a DTC diagnostic model that integrates color Doppler ultrasound signs with laboratory indicators.

Methods and data

Clinical data collection

In this retrospective study, we analyzed patients with thyroid nodules who underwent ultrasonography at Yulin Hospital from February 2021 to March 2023.

This study was approved by the Yulin Hospital Medical Ethics Committee.

Inclusion exclusion criteria

Inclusion criteria: (1) Clinical examination met the diagnostic criteria for thyroid nodules, PTC, and FTC [16]; (2) Age ≥18 years; (3) Available color Doppler ultrasound examination data; (4) Available thyroid hormone, VEGF and TSGF test results; (5) Complete admission data.

Exclusion criteria: (1) Patients with a history of thyroid surgery; (2) Patients with severe organ insufficiency, such as liver, kidney; (3) Patients with other primary tumors, autoimmune diseases; (4) Patients with other diseases affecting laboratory indicators.

Diagnostic criteria for PTC and FTC

The diagnostic criteria for thyroid nodules, PTC, and FTC were met through clinical examination. The gold standard for diagnosis was histopathologic examination of surgically excised tissue, confirming the tumor pathology type. For PTC, key histopathological features include papillary structures, psammoma bodies, and distinctive nuclear features. For FTC, diagnostic criteria emphasize capsular and/or vascular invasion. These criteria are supported by the American Thyroid Association guidelines and other literature as definitive diagnostic methods [16].

Patient grouping

Based on the inclusion and exclusion criteria, we categorized 269 eligible patients into two groups: 105 patients with benign nodules and 164 with cancer. Of the cancer group, 59 had FTC and 105 had PTC.

Baseline data and laboratory value collection

Patient-related information was retrieved from electronic medical records and clinic notes, which included demographic and clinical data such as age, gender, and body mass index (BMI). Ultrasound characteristics assessed included borders, morphology, echogenicity, calcification, blood flow, and lymph node zoning. Laboratory values measured during the initial evaluation for thyroid nodules included free triiodothyronine (FT3), free thyroxine (FT4), thyroglobulin (Tg), thyroid-stimulating hormone (TSH), VEGF, and TSGF. The assays used were electrochemiluminescence for FT3, FT4, Tg, and TSH (Roche-601), and enzyme-linked immunosorbent assays for VEGF and TSGF (Shanghai, China, ml064281 and ml058329, respectively).

Diagnostic feature screening

Using logistic regression, we identified independent diagnostic factors for FTC. This analysis focused exclusively on the cohorts with PTC and FTC, aiming to differentiate between these two types of DTC. The study did not include the benign cohort, as the primary objective was to distinguish between the malignant types. Given the clinical and pathologic overlaps between FTC and PTC, and their shared dependence on TSH, this differentiation is essential for precise therapeutic planning.

Observed data

The observation indicators included: 1. Comparison of baseline data and laboratory indicators between the nodule group and the cancer group. 2. Differentiation of baseline data and laboratory indicators between patients with PTC and FTC. 3. Evaluation of each indicator's diagnostic value for benign nodules versus DTC, and PTC versus FTC using receiver operating characteristic (ROC) curves. 4. Identification of independent diagnostic factors for FTC through logistic regression. 5. Construction of a diagnostic nomogram for FTC using identified independent factors. 6. Assessment of the model's clinical value and stability through decision curve analysis (DCA) and calibration curves. 7. Validation of the model through random patient selection (**Figure 1**).

Statistical analysis

Data processing was conducted using SPSS version 26.0. The Kolmogorov-Smirnov test was employed to analyze measured data. Normally distributed data were presented as mean ± standard deviation (SD), analyzed using independent samples t-tests. Non-normally distributed data were expressed as medians and interquartile ranges (P50 [P25, P75]), with the Mann-Whitney U test applied for analysis. Categorical data comparisons were conducted using the chi-square (χ^2) test. Logistic regression was used to identify independent diagnostic factors for FTC. Nomograms were constructed for these factors, and their calibration and clinical utility were evaluated using DCA curves, calibration plots, and Hosmer-Lemeshow tests. Nomograms were plotted using the R software 'rms' package. A *p*-value <0.05 was considered significant.

Results

Comparison of baseline information

Differences in baseline information between the nodule group and the cancer group were examined. No significant differences were found in age, gender, or BMI between the groups (all P>0.05). However, ultrasound signs including border (P<0.001), morphology (P=0.009), echogenicity (P<0.001), calcification (P=0.001), blood flow (P=0.045), and zoning of enlarged lymph nodes (P=0.003) showed significant differences between the nodule and cancer groups (**Table 1**).

Comparison of laboratory indexes between nodule and cancer groups

Comparative analysis of laboratory indices between the nodule and cancer groups revealed that levels of FT3, FT4, Tg, TSH, VEGF, and TSGF were significantly lower in the nodule group than in the cancer group, with all *P*-values <0.001 (**Table 2**).

Diagnostic value of ultrasound signs and laboratory indices in patients with cancer

ROC curve analysis was used to evaluate the effectiveness of ultrasound signs and laboratory indicators in differentiating benign nodules from DTC. All ultrasound signs, except for bor-

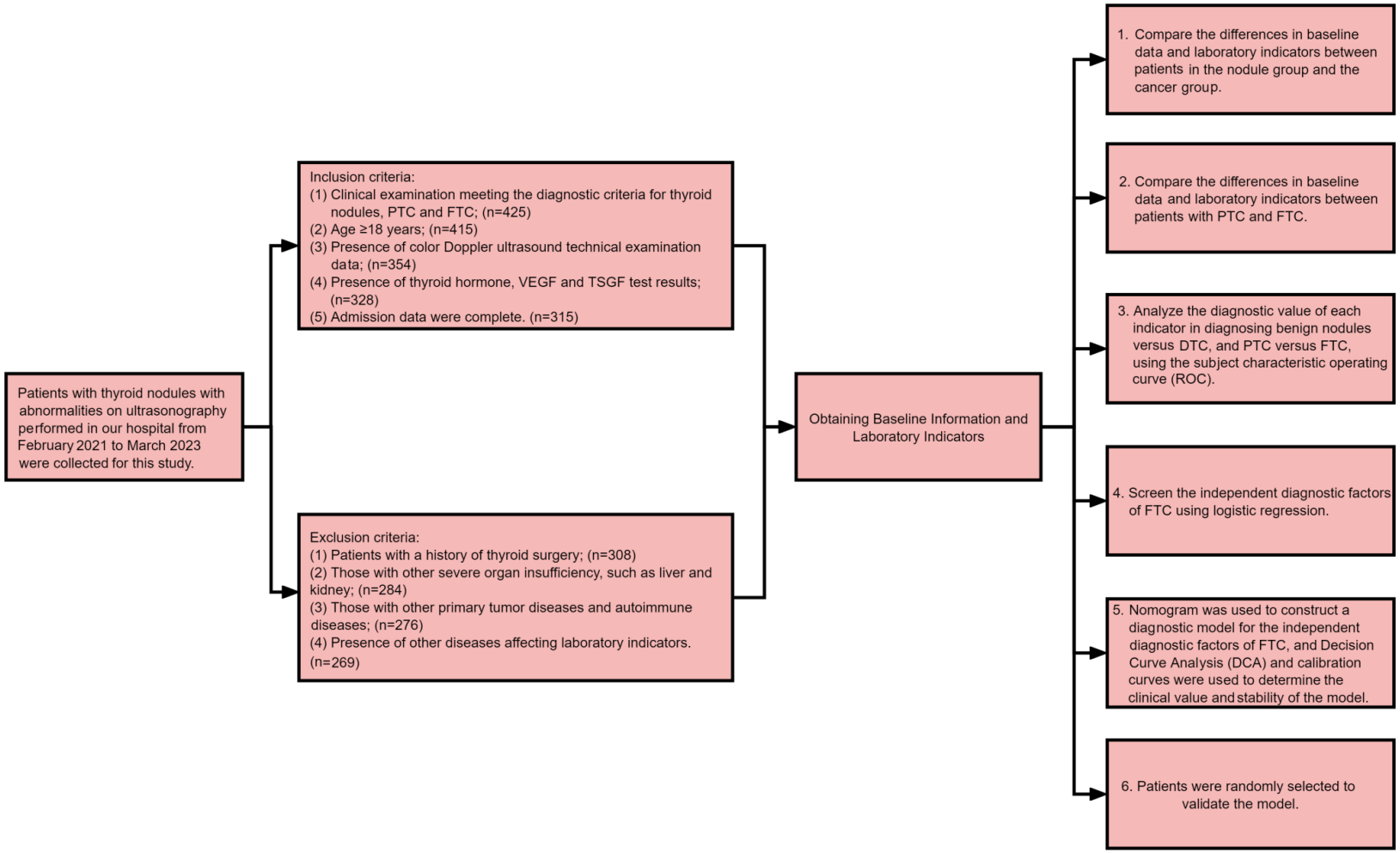

Figure 1. Integration of clinical and laboratory data in the construction and validation of a nomogram for thyroid nodule diagnosis.

Table 1. Comparison of baseline data between nodule and cancer groups

Consideration	Nodule group (n=105)	Cancer group (n=164)	Statistic	*P*-value
Age (years)	46.46±10.15	46.80±10.52	0.27	0.787
Gender				
Male	42 (40.00%)	74 (45.12%)	0.685	0.408
Female	63 (60.00%)	90 (54.88%)		
BMI (kg/m^2)	22.91±5.00	23.46±4.93	0.885	0.377
Border				
Clearer	85 (80.95%)	44 (26.83%)	75.133	<0.001
Unclear	20 (19.05%)	120 (73.17%)		
Morphology				
Aspect ratio <1	69 (65.71%)	81 (49.39%)	6.915	0.009
Aspect ratio ≥1	36 (34.29%)	83 (50.61%)		
Echogenicity				
Low echo	40 (38.10%)	131 (79.88%)	48.257	<0.001
Non-low echo	65 (61.90%)	33 (20.12%)		
Calcification				
Calcification	50 (47.62%)	113 (68.90%)	12.140	0.001
without Calcification	55 (52.38%)	51 (31.10%)		
Blood flow				
No	49 (46.67%)	97 (59.15%)	4.017	0.045
Yes	56 (53.33%)	67 (40.85%)		
Zoning of enlarged lymph nodes				
Single-issue Area	73 (69.52%)	84 (51.22%)	8.826	0.003
Area of common occurrence	32 (30.48%)	80 (48.78%)		

Note: BMI, Body Mass Index.

Table 2. Comparison of laboratory indicators between nodule and cancer groups

Variable	Method	Nodule group (n=105)	Cancer group (n=164)	Statistic	*P*-value
FT3 (pmol/L)	t-test	5.17±1.11	6.97±1.86	9.918	<0.001
FT4 (pmol/L)	t-test	11.33±4.23	17.16±4.68	10.583	<0.001
Tg (ng/mL)	t-test	92.11±14.74	132.65±25.06	16.697	<0.001
TSH (mIU/L)	Mann-Whitney U	1.59 [1.20, 2.04]	2.26 [1.68, 2.62]	6.284	<0.001
VEGF (pg/mL)	t-test	15.88±5.28	24.58±7.47	11.175	<0.001
TSGF (μg/mL)	t-test	50.38±9.81	65.24±11.20	11.46	<0.001

Note: FT3, Free Triiodothyronine; FT4, Free Thyroxine; Tg, Thyroglobulin; TSH, Thyroid-Stimulating Hormone; VEGF, Vascular Endothelial Growth Factor; TSGF, Tissue Specific Growth Factor.

der and echogenicity, showed area under the curves (AUCs) greater than 0.7 (**Table 3**; **Figure 2**). Among laboratory indicators, the AUCs for FT3, FT4, Tg, TSH, VEGF, and TSGF in distinguishing benign nodules from DTC were all above 0.75, with Tg reaching as high as 0.91 (**Table 3**; **Figure 3**).

Comparison of baseline information between PTC and FTC groups

Further analysis comparing baseline data between patients with PTC and FTC found no statistically significant differences in age, gender, BMI, blood flow, or zonation of enlarged lymph nodes (all P>0.05, **Table 4**). However, significant differences were observed in border (P<0.001), morphology (P<0.001), echogenicity (P=0.004), and calcification (P=0.007) between the FTC and PTC groups (**Table 4**).

Comparison of laboratory indexes between FTC and PTC groups

Comparative analysis of laboratory values between FTC and PTC revealed no significant

Table 3. Values of the ROC curve in the diagnosis of benign nodules and DTCs

Predictor variable	Area under the curve	95% CI	Cut-off value	Sensitivity	Specificity	Accuracy	Youden index
Boundary	0.771	0.720-0.821	0.5	73.17%	80.95%	76.21%	54.12%
Morphology	0.582	0.522-0.641	0.5	50.61%	65.71%	56.51%	16.32%
Echo	0.709	0.653-0.765	0.5	79.88%	61.91%	72.86%	41.78%
Calcification	0.606	0.547-0.666	0.5	68.90%	52.38%	62.45%	21.28%
Blood flow	0.562	0.501-0.623	0.5	59.15%	53.33%	56.88%	12.48%
Enlarged lymph node zoning	0.592	0.534-0.650	0.5	48.78%	69.53%	56.75%	18.30%
FT3 (pmol/L)	0.789	0.736-0.843	6.42	61.59%	90.48%	72.86%	52.06%
FT4 (pmol/L)	0.82	0.770-0.869	13.545	76.83%	69.52%	73.98%	46.35%
Tg (ng/mL)	0.91	0.877-0.944	118.94	73.17%	96.19%	82.16%	69.36%
TSH (mIU/L)	0.727	0.667-0.787	2.135	56.10%	79.05%	65.06%	35.15%
VEGF (pg/mL)	0.826	0.778-0.874	20.08	73.78%	75.24%	74.35%	49.02%
TSGF (μg/mL)	0.846	0.799-0.893	58.715	72.56%	83.81%	76.95%	56.37%

Note: DTC, Differentiated thyroid carcinoma; FT3, Free Triiodothyronine; FT4, Free Thyroxine; Tg, Thyroglobulin; TSH, Thyroid-Stimulating Hormone; VEGF, Vascular Endothelial Growth Factor; TSGF, Tissue Specific Growth Factor.

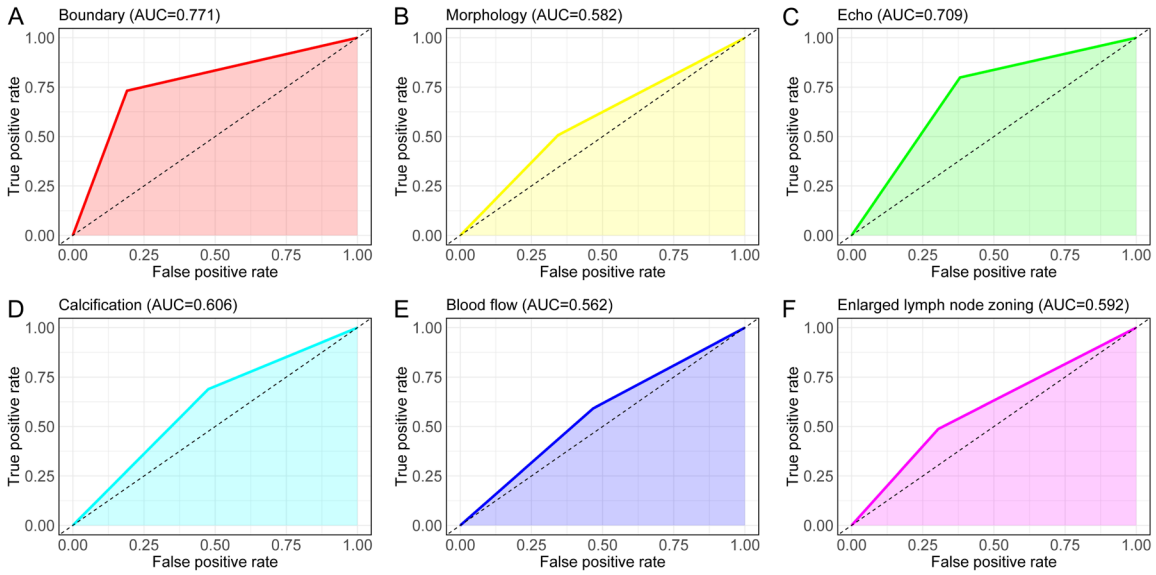

Figure 2. ROC curves of ultrasound signs in the diagnosis of benign nodules versus DTC. A. ROC curves of ultrasound boundaries in the diagnosis of benign nodules versus DTC. B. ROC curve of ultrasound morphology in the diagnosis of benign nodules with DTC. C. ROC curve of ultrasound echo in the diagnosis of benign nodules with DTC. D. ROC curve of ultrasound calcification profile in the diagnosis of benign nodules with DTC. E. ROC curve of ultrasound blood flow profile in the diagnosis of benign nodules with DTC. F. ROC curve of ultrasound enlarged lymph node zoning in the diagnosis of benign nodes with DTC. Note: ROC, Subject characteristic operating curve.

differences in FT3, FT4, or TSH levels between the two groups (all P>0.05, **Table 5**). However, significant increases were observed in Tg (P=0.014), VEGF (P<0.001), and TSGF (P<0.001) in FTC patients compared to PTC patients (**Table 5**).

Logistic regression screening for FTC diagnostic features

Logistic regression analysis was employed to identify diagnostic features that differentiate between PTC and FTC. Continuous variables

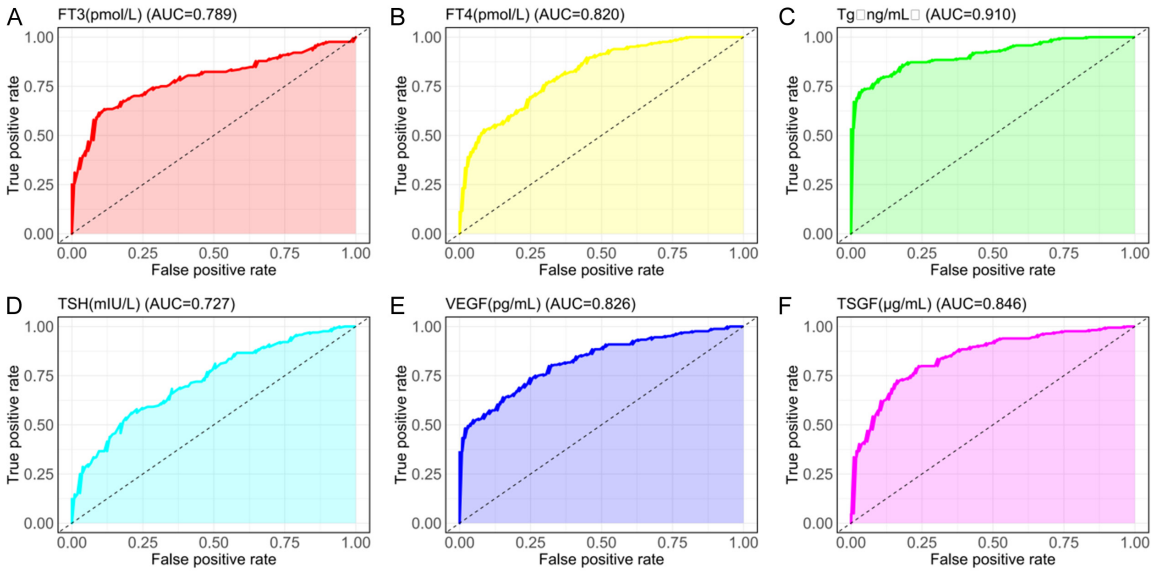

Figure 3. ROC curves of laboratory indices in the diagnosis of benign nodules and DTC. A. ROC curve of FT3 in the diagnosis of benign nodules and DTC. B. ROC curve of FT4 in the diagnosis of benign nodules and DTC. C. ROC curve of Tg in the diagnosis of benign nodules and DTC. D. ROC curve of TSH in the diagnosis of benign nodules and DTC. E. ROC curve of VEGF in the diagnosis of benign nodules with DTC. F. ROC curve for TSGF in the diagnosis of benign nodules vs. DTC. Note: DTC, Differentiated Thyroid Cancer; ROC, Subject Characterization Working Curve; FT3, Free Triiodothyronine; FT4, Free Thyroxine; Tg, Thyroglobulin; TSH, Thyroid-Stimulating Hormone; VEGF, Vascular Endothelial Growth Factor; TSGF, Tissue-Specific Growth Factor.

Table 4. Comparison of baseline data between FTC and PTC groups

Consideration	FTC (n=59)	PTC (n=105)	Statistic	*P*-value
Age (years)	46.81±10.04	46.80±10.82	-0.008	0.994
Gender				
Male	25 (42.37%)	49 (46.67%)	0.281	0.596
Female	34 (57.63%)	56 (53.33%)		
BMI (kg/m^2)	22.65±4.95	23.92±4.89	1.580	0.117
Border				
Clearer	25 (42.37%)	19 (18.1%)	11.341	<0.001
Unclear	34 (57.63%)	86 (81.9%)		
Morphology				
Aspect ratio <1	40 (67.8%)	41 (39.05%)	12.490	<0.001
Aspect ratio ≥1	19 (32.2%)	64 (60.95%)		
Echogenicity				
Low echo	40 (67.8%)	91 (86.67%)	8.368	0.004
Non-low echo	19 (32.2%)	14 (13.33%)		
Calcification				
Calcification	33 (55.93%)	80 (76.19%)	7.235	0.007
Without calcification	26 (44.07%)	25 (23.81%)		
Blood flow				
No	36 (61.02%)	61 (58.10%)	0.133	0.715
Yes	23 (38.98%)	44 (41.90%)		
Zoning of enlarged lymph nodes				
Single-issue Area	33 (55.93%)	51 (48.57%)	0.819	0.365
Area of common occurrence	26 (44.07%)	54 (51.43%)		

Note: BMI, Body Mass Index; FTC, Follicular Thyroid Carcinoma; PTC, Papillary Thyroid Carcinoma.

Table 5. Comparison of laboratory indicators between FTC and PTC groups

Variable	Method	FTC (n=59)	PTC (n=105)	Statistic	*p*_value
FT3 (pmol/L)	t-test	6.73±1.72	7.10±1.92	1.262	0.209
FT4 (pmol/L)	t-test	17.19±4.48	17.14±4.82	-0.067	0.947
Tg (ng/mL)	t-test	138.73±21.44	129.24±26.36	-2.501	0.014
TSH (mIU/L)	t-test	2.19±0.60	2.15±0.67	-0.44	0.661
VEGF (pg/mL)	t-test	28.58±6.87	22.33±6.86	-5.591	<0.001
TSGF (μg/mL)	t-test	69.36±9.61	62.93±11.41	-3.834	<0.001

Note: FT3, Free Triiodothyronine; FT4, Free Thyroxine; Tg, Thyroglobulin; TSH, Thyroid-Stimulating Hormone; VEGF, Vascular Endothelial Growth Factor; TSGF, Tissue Specific Growth Factor; FTC, Follicular Thyroid Carcinoma; PTC, Papillary Thyroid Carcinoma.

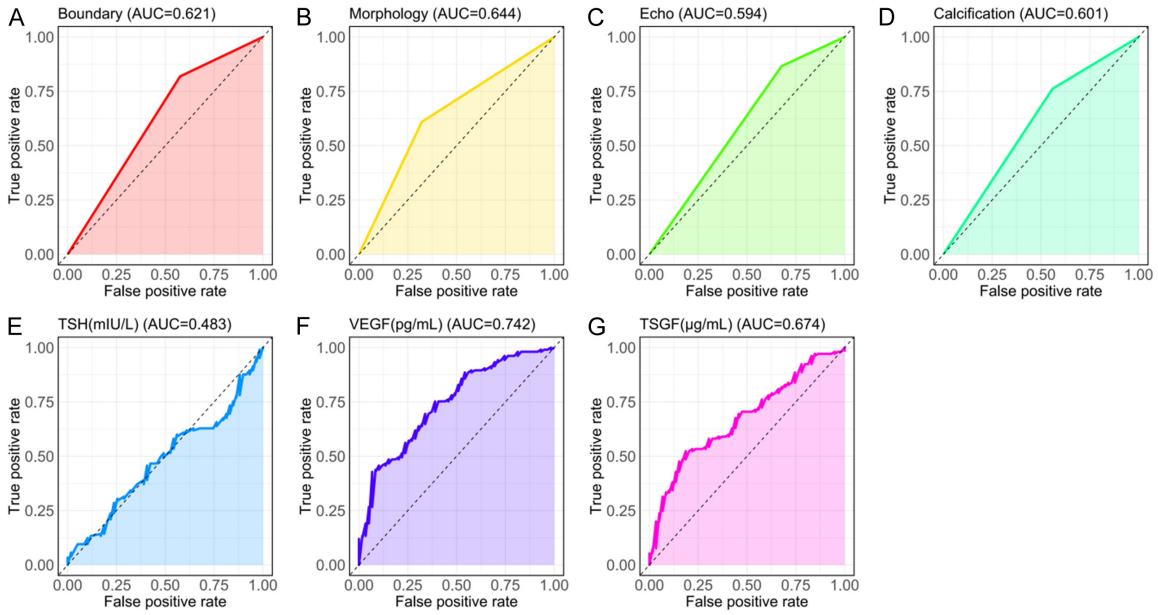

Figure 4. ROC curves of ultrasound signs and laboratory indices in the diagnosis of benign nodules and DTC. A. ROC curves of ultrasound borders in the diagnosis of PTC and FTC. B. ROC curves of ultrasound morphology in the diagnosis of PTC and FTC. C. ROC curves of ultrasound echo in the diagnosis of PTC and FTC. D. ROC curves of ultrasound calcification status in the diagnosis of PTC and FTC. E. ROC curves of TSH in the diagnosis of ROC curves in PTC and FTC. F. ROC curves of VEGF in the diagnosis of PTC and FTC. G. ROC curves for TSGF in the diagnosis of PTC and FTC. Note: DTC, Differentiated Thyroid Cancer; PTC, Papillary Thyroid Cancer; FTC, Follicular Thyroid Cancer; ROC, Subject Characterization Operating Curve; TSH, Thyroid-Stimulating Hormone; VEGF, Vascular Endothelial Growth Factor; TSGF, Tissue Specific Growth Factor.

Table 6. Assignment table

Variable	Assignment content
Boundary	Clearer =1, Unclear =0
Morphology	≤1=1, >1=0
Echo	Low echo =1, Non-low echo =0
Calcification	Calcification =1, without calcification =0
TSH	<2.565=1, ≥2.565=0
VEGF	<26.425=1, ≥26.425=1
TSGF	<62.43=1, ≥62.43=1

Note: TSH, Thyroid-Stimulating Hormone; VEGF, Vascular Endothelial Growth Factor; TSGF, Tissue Specific Growth Factor.

were dichotomized using cut-off values from ROC curves, assigning categorical values to these variables (**Figure 4**; **Table 6**). The analysis identified boundary (P=0.015, OR=0.366), morphology (P=0.012, OR=0.351), echogenicity (P=0.043, OR=2.854), VEGF (P<0.001, OR=0.210), and TSGF (P=0.001, OR=0.220) as independent diagnostic factors for FTC (**Tables 7**, **8**).

FTC nomogram diagnostic model construction

To aid clinicians, a nomogram was constructed for visualizing the diagnostic model of FTC. This

Table 7. Univariate analysis

Variable	Beta value	Std Error	*P* Value	OR Value	95% Lower	95% Upper
Boundary	-1.202	0.366	0.001	0.300	0.145	0.611
Morphology	-1.190	0.343	0.001	0.304	0.153	0.589
Echo	1.127	0.400	0.005	3.087	1.419	6.875
Calcification	0.925	0.348	0.008	2.521	1.277	5.023
TSH	0.251	0.367	0.493	1.286	0.634	2.688
VEGF	-1.559	0.350	<0.001	0.210	0.104	0.413
TSGF	-1.569	0.387	<0.001	0.208	0.094	0.432

Note: TSH, Thyroid-Stimulating Hormone; VEGF, Vascular Endothelial Growth Factor; TSGF, Tissue Specific Growth Factor.

Table 8. Multivariate analysis

Variable	Beta value	Std Error	*P* Value	OR Value	95% Lower	95% Upper
Boundary	-1.090	0.447	0.015	0.336	0.137	0.800
Morphology	-1.048	0.419	0.012	0.351	0.150	0.786
Echo	1.049	0.519	0.043	2.854	1.045	8.120
Calcification	0.792	0.424	0.061	2.208	0.965	5.126
VEGF	-1.534	0.413	<0.001	0.216	0.094	0.477
TSGF	-1.516	0.450	0.001	0.220	0.087	0.514

Note: TSH, Thyroid-Stimulating Hormone; VEGF, Vascular Endothelial Growth Factor; TSGF, Tissue Specific Growth Factor.

nomogram integrated the independent diagnostic factors identified through logistic regression, incorporating five features (**Figure 5A**). Each feature was assigned a score, and the total score provides an estimate of risk based on the linear predictive value displayed at the bottom. The model's efficacy was evaluated using ROC curves, calibration, and DCA. The ROC curve demonstrated an AUC of 0.853, indicating high accuracy (**Figure 5B**). The calibration curve showed excellent agreement between the model-predicted probabilities and the actual observed probabilities, confirming the model's accuracy (**Figure 5C**). The C-index was 0.833 (0.768-0.897), with a goodness-of-fit chi-square of 2.356 and a *P*-value of 0.968, suggesting the model's stability. DCA revealed beneficial outcomes within a threshold range of 1%-95%, with a maximum benefit of 35.32% (**Figure 5D**).

Comparative analysis of the diagnostic efficacy of nomograms and separate indicators

At the study's conclusion, the Delong test was used to compare the diagnostic efficacy between the nomogram and each individual indicator. The nomogram demonstrated significantly higher diagnostic performance compared to each individual indicator including Boundary (P=0.001), Morphology (P< 0.001), Echo (P=0.007), Calcification (P=0.009), TSH (P< 0.001), VEGF (P<0.001), and TSGF (P<0.001) (**Table 9**). In a practical scenario, two randomized patient profiles - one representing a typical PTC patient and the other an FTC patient - were analyzed using the nomogram. In patients with PTC, ultrasound images typically showed poorly defined borders and an aspect ratio of less than 1, alongside hypoechoic features. These patients had VEGF levels at 33.53 pg/mL and TSGF levels at 71.87 μg/mL, leading to a total calculated score of 171. The probability of these patients being diagnosed with FTC was 38%. In contrast, patients with FTC had well-defined borders, an aspect ratio of <1, and non-hypoechoic features.

Their VEGF levels were slightly higher at 35.49 pg/mL, with TSGF also measured at 71.87 μg/mL. This resulted in a higher total patient score of 276, correlating with a 62% likelihood of the FTC diagnosis (**Figure 5A**).

Discussion

Pathologic puncture biopsy remains a primary method for diagnosing DTC, but this invasive technique may yield biased results due to sampling limitations [17]. Fortunately, advancements in medical imaging have made ultrasonography the preferred method for DTC diagnosis due to its cost-effectiveness, non-invasiveness, ease of operation, and high sensitivity [18]. However, ultrasound may present complex features in some tumor cases, complicating accurate identification based solely on subjective assessment. It has been reported that integrating diagnostic ultrasound with laboratory markers significantly enhances the clinical diagnostic accuracy for DTC [19].

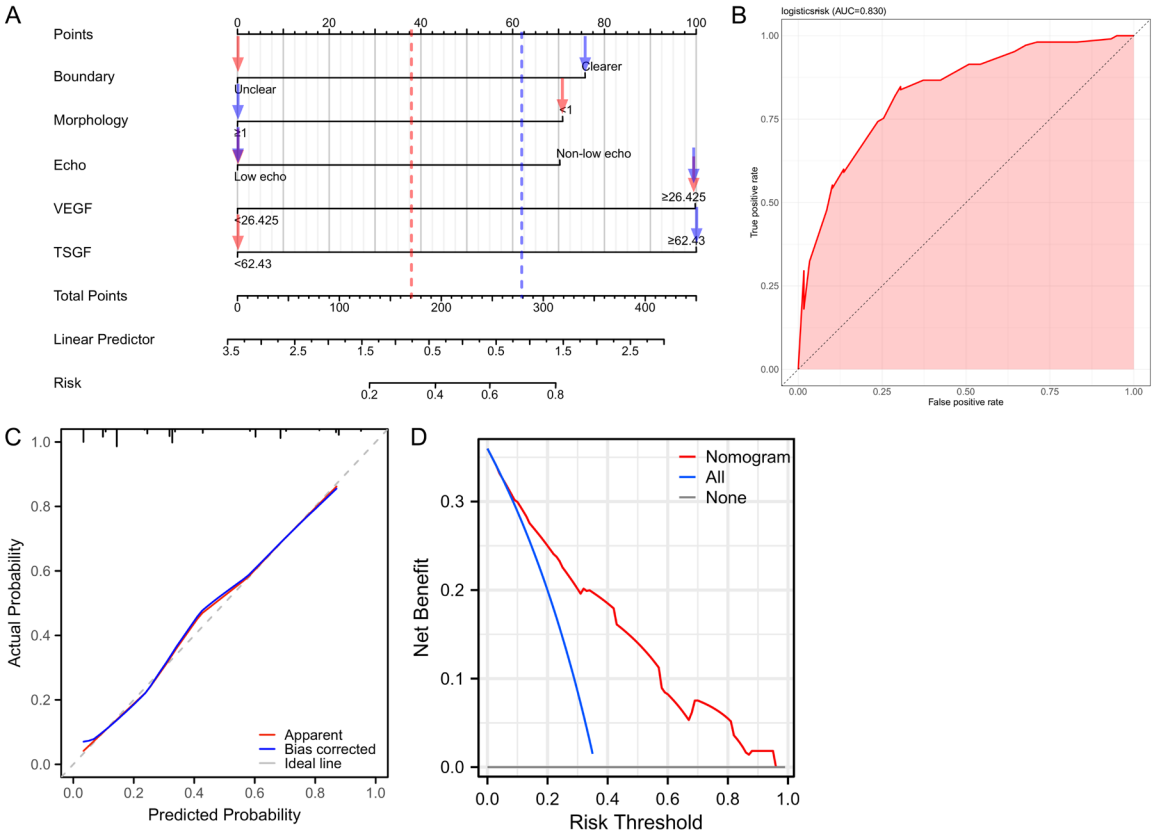

Figure 5. Diagnostic Model Construction of FTC Nomogram. A. Nomogram diagnostic model construction. B. ROC curves to assess the efficacy of nomogram diagnostic models. C. Calibration curve to assess the stability of the nomogram diagnostic model. D. DCA curve to assess the clinical value of the nomogram diagnostic model. Note: FTC, Follicular Thyroid Cancer; ROC, Subject Characteristics Working Curve; DCA, Decision Curve Analysis. The red arrows indicate PTC patients, and the blue arrows indicate FTC patients.

Table 9. Delong test comparing risk models with separate indicators in distinguishing PTC and FTC

Variable 1	Variable 2	Test Methods	Statistic	*P*-value
Boundary	Nomogram	DeLong's test	-3.2341	0.001
Morphology	Nomogram	DeLong's test	3.6953	<0.001
Echo	Nomogram	DeLong's test	2.7025	0.007
Calcification	Nomogram	DeLong's test	2.6166	0.009
TSH (mIU/L)	Nomogram	DeLong's test	-6.276	<0.001
VEGF (pg/mL)	Nomogram	DeLong's test	6.1021	<0.001
TSGF (μg/mL)	Nomogram	DeLong's test	4.0867	<0.001

Note: TSH, Thyroid-Stimulating Hormone; VEGF, Vascular Endothelial Growth Factor; TSGF, Tissue Specific Growth Factor.

In this study, we analyzed the diagnostic value of ultrasound signs combined with laboratory indices for DTC, uncovering statistically significant differences through data analysis. Ultrasound signs such as border definition, morphology, echogenicity, calcification, blood flow, and zoning of enlarged lymph nodes differed significantly between the nodule and cancer groups. Additionally, laboratory values including FT3, FT4, Tg, TSH, VEGF, and TSGF were substantially lower in the nodule group compared to those in the cancer group. These disparities might be indicative of thyroid cancer development, thereby aiding physicians in more accurately diagnosing DTC in clinical settings.

Previous studies corroborate our findings. Li et al. [20] identified specific ultrasound features associated with thyroid cancer development. Fan et al. [21] noted that factors such as nodule size, inhomogeneous enhancement, hypoenhancement, and unclear borders after contrast-enhanced ultrasound were independently significant for diagnosing thyroid cancer. Moreover, Liang et al. [22] emphasized the clinical relevance of detecting serum markers in differenti-

ating thyroid cancer from benign thyroid nodules and distinguishing benign nodules from healthy individuals.

We extended these insights by examining differences between ultrasound signs and labo ratory indicators for diagnosing DTC versus benign nodules using ROC curves. Our analysis revealed substantial diagnostic value in specific ultrasound signs and laboratory indicators. All ultrasound features, except for border clarity and echogenicity, showed AUC values exceeding 0.7, highlighting their diagnostic importance. Among the laboratory indices, FT3, FT4, Tg, TSH, VEGF, and TSGF all had AUC values above 0.75, with Tg showing particularly high diagnostic efficacy (AUC of 0.91).

Accurate diagnosis of thyroid cancer is crucial for effective treatment planning. FTC and PTC, the two prevalent forms of DTC, often show similarities in clinical presentation, pathologic features, and therapeutic approaches, complicating differential diagnosis [23, 24]. In this study, logistic regression identified boundary clarity, morphology, echogenicity, VEGF, and TSGF as independent diagnostic features for FTC. Notably, VEGF showed an AUC of 0.724. Ultrasound parameters critical for evaluating thyroid tumors include boundary clarity - defining the demarcation line between the tumor and surrounding tissues - and morphology, which describes the tumor's structural characteristics [25]. Typically, PTCs present with more irregular or indistinct borders compared to FTCs, and their echogenic properties differ; PTCs are usually hypoechoic, while FTCs may appear more homogeneous or non-hypoechoic [26].

VEGF is known for its role in angiogenic signaling, regulating endothelial cell proliferation and vascular remodeling - critical for tumor cell proliferation, infiltration, and metastasis [27]. Similarly, TSGF promotes vascular network formation within tumor tissues [28]. Prior research indicates that VEGFA protein levels are higher in thyroid cancer than in benign tissues, underscoring its potential as a biomarker [29, 30]. Additionally, Xu et al. [31] suggested that TSGF could predict lymph node metastasis in PTC patients.

Our study developed a nomogram diagnostic model for FTC, integrating five variables: boundary, morphology, echogenicity, VEGF, and TSGF. This model achieved an AUC of 0.853, demonstrating high clinical utility and stability. Lin et al. [32] achieved an AUC of 0.79 with a machine-learning-based FTC diagnostic model, and Yao et al. [33] identified cg06928209 as a candidate molecular marker for FTC, achieving an AUC of 0.77 through DNA methylation and gene expression analysis. However, no models have been established for differentiating PTC from FTC.

Validation using case data from randomly selected PTC and FTC patients confirmed the model's accuracy, reflecting a 38% probability of diagnosing FTC in PTC patients and a 62% probability in FTC patients, aligning closely with pathological diagnoses.

The study, however, was limited by an insufficient sample size, lack of external dataset validation, and absence of long-term follow-up data. Future validation efforts will expand the sample size across diverse regions and ethnicities, validate the model with independent datasets from various healthcare organizations, and establish a long-term follow-up mechanism to gather crucial prognostic information.

In conclusion, our study successfully constructed a nomogram model combining ultrasound signs and laboratory indexes, significantly enhancing the diagnostic accuracy for FTC and providing a robust diagnostic tool for clinical use.

Acknowledgements

Study on the diagnostic value of multimodal ultrasound combined with FNA for papillary thyroid carcinoma (No. YF-2022-48).

Disclosure of conflict of interest

None.

Address correspondence to: Mihong Bai, Department of Laboratory, Baoji People's Hospital, No. 24 Xinhua Lane, Jing'er Road, Weibin District, Baoji 721000, Shaanxi, China. E-mail: 442533446@qq.com

References

[1] Miller KD, Nogueira L, Devasia T, Mariotto AB, Yabroff KR, Jemal A, Kramer J and Siegel RL.

Cancer treatment and survivorship statistics, 2022. CA Cancer J Clin 2022; 72: 409-436.
[2] Miller KD, Fidler-Benaoudia M, Keegan TH, Hipp HS, Jemal A and Siegel RL. Cancer statistics for adolescents and young adults, 2020. CA Cancer J Clin 2020; 70: 443-459.
[3] Chen DW, Lang BHH, McLeod DSA, Newbold K and Haymart MR. Thyroid cancer. Lancet 2023; 401: 1531-1544.
[4] Boucai L, Zafereo M and Cabanillas ME. Thyroid cancer: a review. JAMA 2024; 331: 425-435.
[5] Caresio C, Caballo M, Deandrea M, Garberoglio R, Mormile A, Rossetto R, Limone P and Molinari F. Quantitative analysis of thyroid tumors vascularity: a comparison between 3-D contrast-enhanced ultrasound and 3-D power Doppler on benign and malignant thyroid nodules. Med Phys 2018; 45: 3173-3184.
[6] Schlumberger M and Leboulleux S. Current practice in patients with differentiated thyroid cancer. Nat Rev Endocrinol 2021; 17: 176-188.
[7] Liu Z, Wang R, Zhou J, Zheng Y, Dong Y, Luo T, Wang X and Zhan W. Ultrasound lymphatic imaging for the diagnosis of metastatic central lymph nodes in papillary thyroid cancer. Eur Radiol 2021; 31: 8458-8467.
[8] Zhang F, Sun Y, Wu X, Meng C, Xiang M, Huang T, Duan W, Wang F and Sun Z. Analysis of the application value of ultrasound imaging diagnosis in the clinical staging of thyroid cancer. J Oncol 2022; 2022: 8030262.
[9] Pérez-Gutiérrez L and Ferrara N. Biology and therapeutic targeting of vascular endothelial growth factor A. Nat Rev Mol Cell Biol 2023; 24: 816-834.
[10] Bokhari SMZ and Hamar P. Vascular endothelial growth Factor-D (VEGF-D): an angiogenesis bypass in malignant tumors. Int J Mol Sci 2023; 24: 13317.
[11] Nair B, Kuriakose A, Baby B and Nath LR. Tumor-specific growth factor (TSGF): a futuristic tumor biomarker in early diagnosis of cancer. Adv Pharm Bull 2023; 13: 483-488.
[12] Song X, Liang B, Wang C and Shi S. Clinical value of color Doppler ultrasound combined with serum CA153, CEA and TSGF detection in the diagnosis of breast cancer. Exp Ther Med 2020; 20: 1822-1828.
[13] Yin LK, Sun XQ and Mou DZ. Value of combined detection of serum CEA, CA72-4, CA19-9 and TSGF in the diagnosis of gastric cancer. Asian Pac J Cancer Prev 2015; 16: 3867-3870.
[14] Fan XY, You W, Chen Y, Nie CC, Wang XL, Lei C, Song J and Luo HL. A meta-analysis of the value of serum TSH concentration in the diagnosis of differentiated thyroid cancer in patients with thyroid nodules. Heliyon 2024; 10: e24391.
[15] Oskouie AA, Ahmadi MS and Taherkhani A. Identification of prognostic biomarkers in papillary thyroid cancer and developing non-invasive diagnostic models through integrated bioinformatics analysis. Microrna 2022; 11: 73-87.
[16] Perrier ND, Brierley JD and Tuttle RM. Differentiated and anaplastic thyroid carcinoma: major changes in the American Joint Committee on Cancer eighth edition cancer staging manual. CA Cancer J Clin 2018; 68: 55-63.
[17] Ruiz-Pozo VA, Cadena-Ullauri S, Guevara-Ramírez P, Paz-Cruz E, Tamayo-Trujillo R and Zambrano AK. Differential microRNA expression for diagnosis and prognosis of papillary thyroid cancer. Front Med (Lausanne) 2023; 10: 1139362.
[18] Zheng H, Xiao Z, Luo S, Wu S, Huang C, Hong T, He Y, Guo Y and Du G. Improve follicular thyroid carcinoma diagnosis using computer aided diagnosis system on ultrasound images. Front Oncol 2022; 12: 939418.
[19] Chen B, Yan Z, Bao Y, Li J, Luo C, Yang G, Li T, Cheng X and Lv J. Detection of thyroglobulin for diagnosis of metastatic lateral cervical lymph nodes in papillary thyroid carcinoma: accuracy and application in clinical practice. Transl Cancer Res 2024; 13: 1043-1051.
[20] Li W, Gao L, Du Y, Wang Y, Yang X, Wang H and Li J. Ultrasound microflow patterns help in distinguishing malignant from benign thyroid nodules. Cancer Imaging 2024; 24: 18.
[21] Fan J, Tao L, Zhan W, Li W, Kuang L, Zhao Y and Zhou W. Diagnostic value of qualitative and quantitative parameters of contrast-enhanced ultrasound for differentiating differentiated thyroid carcinomas from benign nodules. Front Endocrinol (Lausanne) 2024; 14: 1240615.
[22] Liang JJ, Feng WJ, Li R, Xu RT and Liang YL. Analysis of the value and safety of thyroid-stimulating hormone in the clinical efficacy of patients with thyroid cancer. World J Clin Cases 2023; 11: 1058-1067.
[23] Paudel J. Establishing a cutoff serum thyroglobulin value for the diagnosis and management of well-differentiated thyroid cancer. World J Nucl Med 2023; 22: 208-216.
[24] Tallini G, Tuttle RM and Ghossein RA. The history of the follicular variant of papillary thyroid carcinoma. J Clin Endocrinol Metab 2017; 102: 15-22.
[25] Haymart MR, Banerjee M, Reyes-Gastelum D, Caoili E and Norton EC. Thyroid ultrasound and the increase in diagnosis of low-risk thyroid cancer. J Clin Endocrinol Metab 2019; 104: 785-792.

[26] Bukasa-Kakamba J, Bayauli P, Sabbah N, Bidingija J, Atoot A, Mbunga B, Nkodila A, Atoot A, Bangolo AI and M'Buyamba-Kabangu JR. Ultrasound performance using the EU-TIRADS score in the diagnosis of thyroid cancer in Congolese hospitals. Sci Rep 2022; 12: 18442.
[27] Xin H, Zhong C, Nudleman E and Ferrara N. Evidence for pro-angiogenic functions of VEGF-Ax. Cell 2016; 167: 275-284, e276.
[28] Xu X, Wang W, Tian B, Zhang X, Ji Y and Jing J. The predicting role of serum tumor-specific growth factor for prognosis of esophageal squamous cell carcinoma. BMC Cancer 2023; 23: 1067.
[29] Stuchi LP, Castanhole-Nunes MMU, Maniezzo-Stuchi N, Biselli-Chicote PM, Henrique T, Padovani Neto JA, de-Santi Neto D, Girol AP, Pavarino EC and Goloni-Bertollo EM. VEGFA and NFE2L2 gene expression and regulation by MicroRNAs in thyroid papillary cancer and colloid goiter. Genes (Basel) 2020; 11: 954.
[30] Vela-Gaxha Z, Shahini L and Manxhuka-Kerliu S. The prognostic role of vascular endothelial growth Factor-A expression in thyroid carcinomas. Folia Med (Plovdiv) 2019; 61: 61-68.
[31] Xu X, Wang W, Sun T, Tian B, Du L and Jing J. The predicting role of serum TSGF and sIL-2R for the lymph node metastasis of papillary thyroid carcinoma. Dis Markers 2022; 2022: 3730679.
[32] Lin AC, Liu Z, Lee J, Ranvier GF, Taye A, Owen R, Matteson DS and Lee D. Generating a multimodal artificial intelligence model to differentiate benign and malignant follicular neoplasms of the thyroid: a proof-of-concept study. Surgery 2024; 175: 121-127.
[33] Yao Y, Xu P, Ying T, Wang Y, Wang X, Shu L, Mo Z, Chen Z, Wang X, Wang W, Teng L and Lou X. Integrative analysis of DNA Methylation and gene expression identified follicular thyroid cancer-specific diagnostic biomarkers. Front Endocrinol (Lausanne) 2022; 12: 736068.